Frontiers in Bioscience Landmark

Front. Biosci. (Landmark Ed) **2025**; 30(3): 28210
https://doi.org/10.31083/FBL28210

Original Research

CD47 Contributes to the Proliferation of Breast Cancer

Junbin Wang[1,†], Xia Wu[2,†], Xuejian Liu[3,*], Ying Xu[4,*]

[1]The Second Clinical Medicine School, Shandong University of Traditional Chinese Medicine, 250014 Jinan, Shandong, China
[2]Department of Oncology, Shandong Provincial Third Hospital, 250031 Jinan, Shandong, China
[3]Department of General Surgery, The First Rehabilitation Hospital of Shandong, 276000 Linyi, Shandong, China
[4]Department of Breast and Thyroid Surgery, Shandong Provincial Third Hospital, 250031 Jinan, Shandong, China
*Correspondence: liuxj168@sina.com (Xuejian Liu); xuying2205@126.com (Ying Xu)
[†]These authors contributed equally.

Academic Editor: Sung Eun Kim
Submitted: 13 November 2024 Revised: 14 December 2024 Accepted: 30 December 2024 Published: 5 March 2025

Abstract

Background: The *CD47* molecule (*CD47*) performs a novel role in regulating immunoreactions by binding to signal-regulatory protein alpha (*SIRPα*), resulting in the tumorigenesis of multiple malignant neoplasms. However, its effects and mechanisms in breast cancer (BC) remain unknown. **Methods**: To explore the molecular mechanisms and explicit impacts of CD47, we screened two databases for *CD47*-associated signaling pathways and cellular functions. BC samples and patients' basic information were collected to identify the statistical significance of *CD47* expression. We also constructed experiments to validate the regulatory role of *CD47* in BC cell proliferation. **Results**: Analysis of the TCGA-BRCA, GSE42568, and GSE15852 datasets demonstrated an elevated level of *CD47* in BC tissues. A Venn diagram revealed 11,194 co-expressed genes, and pathway analysis linked elevated *CD47* levels to critical signaling pathways, such as cytokine-receptor interactions and Janus kinase/signal transducer and activator of transcription (*JAK/STAT*) signaling, which are integral to cell proliferation and invasiveness. Clinical data from 108 BC specimens showed that *CD47* localization was primarily membranous, with higher levels correlating with proliferation marker Ki-67 (*Ki-67*) expression ($p < 0.0001$) and advanced tumor/node/metastasis (TNM) stage ($p < 0.0001$). Additionally, functional assays demonstrated that *CD47* depletion reduced cell viability ($p < 0.01$), migration ($p < 0.001$), and invasion ($p < 0.05$ in 4T1 cells; $p < 0.001$ in MDA-MB-231 cells) *in vitro* and led to smaller tumor volumes ($p < 0.0001$) *in vivo*. **Conclusion**: *CD47* is a key regulator of BC cell proliferation and invasiveness and serves as a potential marker for assessing tumor aggressiveness and guiding therapeutic strategies.

Keywords: *CD47*; breast cancer; proliferation; tumor progression

1. Introduction

Breast cancer (BC) continues to be one of the most common cancers impacting women around the world, with projections indicating approximately 2.3 million new diagnoses in 2024 [1]; therefore, it continues to represent a significant public health challenge. Recent data have highlighted demographic shifts in BC incidence, particularly an alarming increase among younger women and diverse populations, and disparities in access to healthcare exacerbate outcomes in underrepresented groups. Moreover, the mechanisms of metastasis and invasion in BC involve complex interactions between cancer cells and their microenvironment, contributing to the metastatic cascade [2,3]. Notably, key genes such as BRCA1 DNA repair associated (*BRCA1*) and BRCA2 DNA repair associated (*BRCA2*) have been identified as crucial players in BC development, and mutations in these genes are associated with a significantly increased risk of developing the disease and with aggressive tumor behavior [4]. In response to these challenges, the treatment landscape has evolved to include targeted therapies, such as trastuzumab for Human epithelial receptor-2 (*HER2*)-positive tumors and immunotherapies that show promise in triple-negative BC [5]. Overall, the fight against BC continues to evolve rapidly, and future studies should concentrate on understanding the fundamental mechanisms of metastasis and enhance interventions that are customized for the various populations impacted.

CD47 molecule (*CD47*), a transmembrane protein primarily found on the surface of diverse cells, functions significantly in modulating immune responses. It does this by interacting with signal-regulatory protein alpha (*SIRPα*) present on macrophages, which consequently inhibits phagocytosis and enables cells to avoid immune clearance [6–8]. *CD47* is often up-expressed in carcinomas and contributes to immune evasion and poor prognosis in various cancers, including leukemia, lymphoma, and solid tumors [9]. This overexpression facilitates tumor progression, metastasis, and resistance to therapies, prompting research into *CD47* as a therapeutic target through strategies such as monoclonal antibodies that block its interaction with *SIRPα* [8,10,11]. Although some studies have indicated *CD47* overexpression in specific BC subtypes, its precise involvement and clinical significance in this malignancy remain unclear, necessitating further investigation to elucidate its therapeutic potential and role in BC progression. Overall, the implications of *CD47* in cancer biology

are expanding; however, more research is required to determine its impact, specifically in the context of BC.

Given the unclear applications of *CD47* gene expression in BC, this study conducted an in-depth investigation using several methodologies, including bioinformatics analysis through database retrieval, statistical analysis of clinical sample data, and immunohistochemical staining of tissue samples. By integrating these approaches, our goal was to clarify how *CD47* is expressed in breast cancer and to evaluate its possible significance in relation to disease progression and patient outcomes. These comprehensive analyses support valuable insights into the role of *CD47* in BC and contribute to inform future therapeutic strategies targeting this gene.

2. Materials and Methods

2.1 Data Acquisition and Processing

The Cancer Genome Atlas-Breast Cancer (TCGA-BRCA)-related data were downloaded from the Gene Expression Datasets Associated with BC using the Genomic Data Commons (GDC) data portal (https://portal.gdc.cancer.gov/) and the Gene Expression Omnibus database (https://www.ncbi.nlm.nih.gov/geo/). The analysis of the differential expression of *CD47* in breast cancer and adjacent non-cancerous tissues was conducted using Gene Expression Profiling Interactive Analysis (GEPHIA2; http://gepia2.cancer-pku.cn/).

2.2 Bioinformatic Analysis of Differential Expression Gene (DEGs)

In the TCGA-BRCA, GSE15852, and GSE42568 datasets, using the "DESeq2" software package (dds <- DESeqDataSetFromMatrix (countData, colData, design = ~ condition); alpha = 0.05; lfcThreshold >1; Version 3.0; Michael Love and Wolfgang Huber; London, USA), we screened out the DEGs in the samples with high and low expression of *CD47* in tumor tissues. Venn diagrams showed co-expressed genes, and functional enrichment analysis utilizing Gene Ontology (GO) alongside Kyoto Encyclopedia of Genes and Genomes (KEGG) pathways was conducted through the cluster-Profiler R package 4.3.2 (Michael Love and Wolfgang Huber; NY, USA) [12]. This analysis aimed to categorize a range of biological processes, molecular functions, cellular components, and pathways associated with the identified marker genes within the target clusters [13,14] (**Supplementary Fig. 1A,B**).

2.3 Clinical Samples and Immunohistochemistry (IHC)

This research conducted a retrospective analysis of breast cancer cases stored in the Pathology Department at Shandong Third Hospital from 2020 to 2022. The analysis included 108 patients who had been diagnosed with invasive ductal carcinoma of the breast, all of whom did not receive preoperative chemotherapy, radiotherapy, or endocrine treatment. This study was conducted in accordance with the Declaration of Helsinki and was approved by the relevant ethics committee. The Ethics Committee and Institutional Review Board of the Third Hospital of Shandong Province approved the study, and the necessity for informed consent was signed (No. KYLL-2021066). An immunohistochemical staining assay was used to detect 108 paired BC tissue samples. Rabbit anti-human *CD47* monoclonal antibody was purchased (ab300124, Cell Signaling Technology, Inc. Boston, USA; Dilution concentration: 1:200). Staining results were analyzed using ImageJ software (Version 1.8.0.345; National Institutes of Health; NY, USA) [15] and interpreted according to the semi-quantitative method utilized to assess the expression of *CD47* in BC and paraneoplastic samples.

2.4 Cell Culture

Human BC cells (MDA-MB-231 cell line; ZQ0118) and mouse BC 4T-1 cells (ZQ0201; Shanghai Zhongqiao Xinzhou Biological Company, Shanghai, China) were inoculated in Dulbecco's Modified Eagle Medium (Gibcp 11885084, Suzhou, Jiangsu, China) with 10% fetal bovine serum (Suolaibao technology company, Beijing, China) and 100 IU/mL penicillin/streptomycin at 37 °C with 5% CO_2. All cell lines were validated by STR profiling and tested negative for Mycoplasma.

2.5 Cell Transfection

Cells were placed in six-well plates at a density of 2×10^5 cells per well and allowed to incubate overnight to achieve 90% confluency. For each well, plasmid DNA [2 µg *CD47*-short hairpin RNA (shRNA); D010003, GenePharma company; Shanghai, China] was diluted in 250 µL of DMEM (ZQ-100; Shanghai Zhong Qiao Xin Zhou Biotechnology Co, Shanghai, China) and mixed gently. Separately, 10 µL of transfection reagent (e.g., Lipofectamine 3000, ThermoFisher, Shanghai, China) incubated for 5 min at 24 °C. The diluted DNA and transfection reagent were then combined, incubated for 20 min, and were added dropwise to the cells, which were then incubated at 37 °C in a CO_2 incubator. After 6 hours, the medium was replaced with a fresh fetal medium. Transfection efficiency was assessed 24–48 h post-transfection using quantitative real-time (qPCR) and Western blot (WB) assays (**Supplementary Tables 1,2**).

2.6 Quantitative Real-Time Polymerase Chain Reaction (qRT-PCR)

Total RNA was extracted from cultured cells by Easy Pure RNA Isolation Kit (R0018S; Beyotime Biotechnology, Shanghai, China) and a reverse-transcription (RT) Kit (D7153; BeyoRT M-MuLV, Beyotime Biotechnlogy Company, Shanghai, China). The cDNA was subjected to qRT-PCR with gene-specific primers in the presence of qPCR Master Mix (BeyoRT II cDNA, Beyotime Biotechnlogy Company, Shanghai, China). Relative mRNA expression

levels were calculated using the 2-ΔΔCt method, where ΔCt represents the difference in threshold cycle (Ct) values between the target gene and a reference gene (e.g., *GAPDH* (**Supplementary Table 3**). All samples were analyzed in triplicate.

2.7 Western Blot Assay

The total protein was extracted from the cells using the Radio Immunoprecipitation Assay (RIPA) extraction reagent (Beyotime Biotechnology Company, Shanghai, China), and the protein concentration was determined using a bicinchoninic acid protein assay (Beyotime Biotechnology Company, Shanghai, China). Subsequently, the samples were subjected to sodium dodecyl sulfate-polyacrylamide gel electrophoresis. The primary antibody (anti-CD47:1:2000, 20305–1-AP; anti-β-actin: 1:2000, 10494-1-AP, Proteintech, Rosemont, IL, Beijing, China) and the secondary antibody (IgG-HRP, 1:3000, AS014; Wolburn, Boston, MA, USA) were incubated, respectively. Protein bands were visualized using chemiluminescence and analyzed using the ImageJ software (Version 2.0; available from the National Institutes of Health, USA) (**Supplementary Fig. 2**).

2.8 Cell Counting Kit-8 (CCK8) Assay

Experimental cells were plated in a 96-well plate with a density of 5000 cells per well. The proliferation rates of 4T-1 and MB-231 cells from both the short hairpin (sh)-CD47 and control groups were assessed. Cell viability measurements occurred every 12 hours. Daily, 10 µL of CCK-8 reagent (MCE, Shanghai, China) was added to each well of the 96-well plates and incubated at 37 °C for one hour. Optical density values were then determined using a microplate reader (Infinite® M1000PRO, TECAN, Männedorf, Switzerland) at a 450-nm wavelength.

2.9 Colony Formation Assay

In summary, 400 cells were placed in a six-well plate and allowed to incubate in culture medium containing 10% fetal bovine serum at a temperature of 37 °C with 5% CO_2 for a duration of 2 weeks. The culture medium was replaced every three days. Prior to staining with 0.1% crystal violet, the cells were fixed using 4% paraformaldehyde for 30 minutes. The clones were then quantified using ImageJ software.

2.10 Wound Healing Assay

Cells from each group were inoculated in six-well plates (2×10^5 cells/well). When the cell growth reached 85% confluence, the bottom of the six-well plate was scratched vertically and cultured in Dulbecco's Modified Eagle Medium with DMEM. The scratches were observed under a microscope (Olympus, IX-71, Tokyo, Japan,) and photographed at 0, 24, and 48 h. The healing rate was determined using the formula ((initial scratch area - scratch area at time t)/(initial scratch area)) $\times$ 100%.

2.11 Cell Migration Assay

The capability of cell migration was assessed using 24-well transwell chambers (with an 8-µm pore size; Sigma-Aldrich, Corning, NY, USA). In the upper compartment, 100 µL of serum-free medium was combined with 2×10^4 cells, while the lower compartment contained 600 µL of medium supplemented with 10% fetal bovine serum. Following 48 hours of culture in a 37 °C incubator, the cells were fixed using 4% paraformaldehyde and subsequently treated with 0.4% crystal violet solution (Sigma-Aldrich, V5265, Shanghai, China). The stained cells were then photographed (Olympus, Tokyo, Japan) and quantified.

2.12 Cell Transwell Assay

Culture the cells until they reach 70–80% confluence, then detach and re-suspend them in fresh medium. Use diluted Matrigel (3 mg/mL; M8370, Suolaibao company, Beijing, China) coated on the upper surface of the transwell inserts and add a predetermined number of cells to the upper chamber, while adding complete medium to the lower chamber. This process should be performed on ice, allowing the Matrigel to solidify at 37 °C for 45 minutes. Incubate the setup at 37 °C with 5% CO_2 for 24–48 hours. After incubation, fix the migrated cells on the lower surface of the insert using a fixative solution, followed by staining with a crystal violet. Once stained, rinse to remove excess dye, allow the inserts to dry, and then examine them under a microscope to count the number of invaded cells.

2.13 In Vivo Growth Assays

Female BALB/C nude mice (5-weeks-old; 17.54 $\pm$ 0.867 g; 45 in all; Beijing Viewsolid Biotech Co., Ltd., Beijing, China) were utilized to construct the xenograft model. Knocked-down 4T-1/sh-NC (Negative Control) and 4T-1/sh-CD47 cells were suspended in 100 µL of PBS and injected subcutaneously. Tumors were measured every 2–3 d. After 33 days, mice were euthanized with a 20% concentration of isoflurane (1217828, Shanghai Yuyan Scientific Instrument Co., LTD, Shanghai, China) in airtight equipment for three minutes according to the ethical guidelines [16], and xenograft tumors were dissected for subsequent experiments. All animal experimental processes were approved by the Laboratory Animal Center of Shandong Third Hospital (No. DWKYLL-2021023).

2.14 Statistical Analysis

Statistical analyses were conducted utilizing IBM SPSS Statistics software (IBM Corp., Armonk, NY, USA) version 29.0, along with GraphPad Prism 10.0 (GraphPad Software, La Jolla, CA, USA), and R version 3.6.1 (R Foundation for Statistical Computing, Vienna, Austria) [12]. The results of the IHC were evaluated employing the chi-

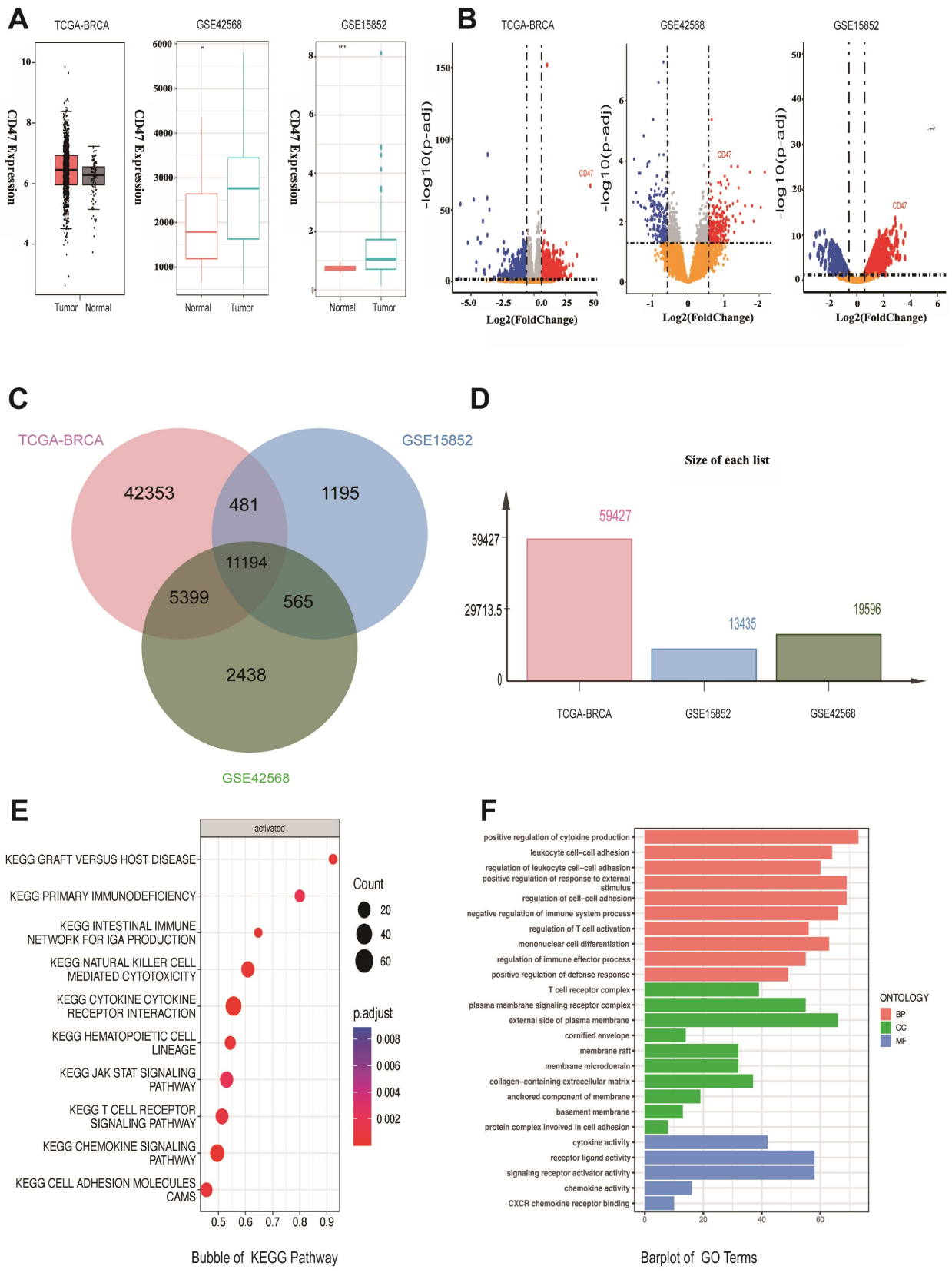

Fig. 1. Bioinformatic analysis of *CD47* in two databases. (A) Column diagrams of *CD47* expression in tumors and normal tissues based on The Cancer Genome Atlas and Gene Expression Omnibus databases. (B) Volcano plots of differentially expressed genes according to three databases. (C) Venn diagram of three databases showing co-expressed genes. (D) Gene numbers in the three databases. (E,F) The Gene Ontology/Kyoto Encyclopedia of Genes and Genomes clustering analysis of high *CD4* expression-associated signaling pathways and functions. BP, Biological Process; CC, Cellular Component; MF, Molecular Function.

Table 1. CD47 expression in cancer and paired para-cancerous tissues by immunohistochemical staining.

	CD47 Expression (n = 109; %)	*T* test	*p* value
Cancer	26.996 ± 0.455	271.200	<0.000
Para-cancer	11.932 ± 0.354		

n = 108. All experiments had three biological replicates with similar results. Data are presented as mean ± standard deviation.

square test. A *p*-value of less than 0.05 was deemed statistically significant. To compare the two sample groups, an independent samples *t*-test was used, whereas a one-way *ANOVA* was applied for comparisons involving multiple groups. Following one-way *ANOVA*, post-hoc multiple comparisons were performed using the Tukey's HSD (Honestly Significant Difference) test to evaluate differences between group means. This method was chosen for its ability to control the Type I error rate while comparing all pairs of means. All statistical tests were two-sided, and each experiment was conducted three times for every group.

3. Results

3.1 Bioinformatic Information of CD47 in Breast Cancer

To elucidate the divergence in *CD47* expression in BC, we analyzed two datasets derived from *TCGA-BRCA* databases: GSE42568 and GSE15852. Our findings indicated that *CD47* expression was significantly high in BC samples comparing to normal breast samples (Fig. 1A,B). Subsequently, we used a Venn gram to identify approximately 11,194 genes co-expressed across the three datasets (Fig. 1C,D). To conduct a comprehensive analysis of the signaling pathways correlated to the regulation of activated *CD47* from KEGG database [13], we established that elevated *CD47* levels in BC were linked to several critical pathways, including cytokine-cytokine receptor interactions, the *JAK/STAT* signaling pathway, chemokine signaling pathway, and cell adhesion molecule pathways. These pathways are pivotal in driving processes such as cell proliferation, apoptosis, metabolism, and invasiveness (Fig. 1E; **Supplementary Fig. 3**). Additionally, the GO analysis indicated that differentially expressed genes (DEGs) associated with elevated *CD47* expression were connected to the enhancement of cytokine production, activity of receptor ligands, and the activation of signaling receptors (Fig. 1F).

3.2 The Significance of CD47 in Clinical Breast Cancer

To investigate the relationship between *CD47* level and BC, we collected data from 108 clinical cases between January 2020 and January 2022. IHC staining demonstrated that *CD47* was primarily localized on the membrane of BC cells, and these levels were significantly higher in cancer tissues than in para-cancerous tissues (Fig. 2A,B; Table 1; $p < 0.0001$). Furthermore, statistical analyses uncovered that increased *CD47* expression was associated with several factors, including high *Ki-67* levels, age >60 years, and TNM stage. Nevertheless, there were no statistically significant differences in *CD47* levels between the estrogen receptor-, progesterone receptor, or Human Epidermal Growth Factor Receptor-positive and negative groups (Table 2).

Table 2. Clinical basic information was associated with CD47 expression.

	N	CD47 Expression (%)	*T/F* test	*p* value
Age (years)				
<60	47	28.709 ± 1.965	9.048	<0.000
≥60	61	26.362 ± 0.442		
ER				
Positive	79	26.997 ± 0.455	0.130	0.896
Negative	29	27.046 ± 3.288		
PR				
Positive	67	28.708 ± 1.965	1.760	0.081
Negative	41	28.023 ± 1.906		
HER-2				
Positive	62	27.268 ± 0.838	0.330	0.272
Negative	46	27.226 ± 0.131		
Ki-76				
<20%	32	25.930 ± 0.103	11.580	<0.000
≥20%	76	26.997 ± 0.455		
pTNM stage				
I	32	25.930 ± 0.103	9.557	<0.000
II	45	26.591 ± 0.767		
III	13	26.020 ± 1.837		
IV	18	25.414 ± 0.626		

ER, estrogen receptor; PR, progesterone receptor; HER-2, Human Epidermal Growth Factor Receptor-2; pTNM stage, pathological tunor/node/metastasis (TNM) staging; I, $T_1N_0M_0$; II, $T_2N_0M_0/T_2N_1M_0/T_3N_{0-3}M_0$; III, $T_3N_{0-3}M_0/T_4N_{0-3}M_0$; IV, M_1. All experiments had three biological replicates with similar results. Data are presented as mean ± standard deviation.

3.3 CD47 Maintained the Proliferation of Breast Cancer

We performed *in vitro* and *in vivo* experiments to verify the function of *CD47* in BC. Given the elevated levels of *CD47*, we transfected three shRNA plasmids into 4T1 and MB-231 cells to downregulate *CD47* expression (**Supplementary Fig. 1**). Notably, cell viability was overtly lower in the sh-CD47 group than that in the control group, which was further corroborated by monoclonal proliferation results using CCK-8 staining (Fig. 3). The wound healing assay results for 4T1 and MB-231 cells demonstrated that the migratory ratios at 24 and 48 hours were reduced in the sh-CD47 group compared with the control groups ($p < 0.0001$; Fig. 4A–D). Combined with the outcomes of the cell migration assay, the invasive ability of sh-CD47 cancer cells decreased compared to that of normal cancer cells ($p < 0.05$ in 4T1 cells; $p < 0.001$ in MB-231 cells; Fig. 4E,F). Furthermore, we established subcutaneous tumors in nude mice using sh-CD47 4T1, control

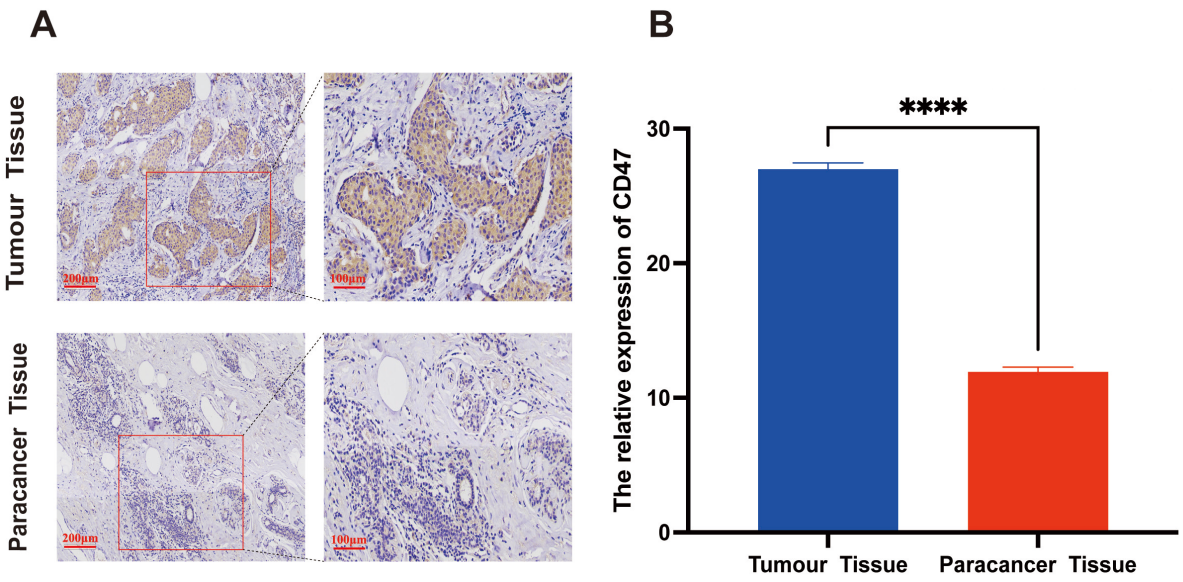

Fig. 2. The clinical significance of *CD47* expression in breast cancer. (A,B) CD47 expression in cancer and paired para-cancerous tissues by immunohistochemical staining. The scale bar = 100 or 200 μm. All experiments had three biological replicates with similar results. Data are presented as mean ± standard deviation. ****$p \leq 0.0001$.

4T1, and 4T1 cells with empty plasmids. The results indicated that the tumor volume was distinctly lower in the sh-CD47 group than that in the other two groups (Fig. 5A–E). In terms of the proliferative markers, Cyclin dependent kinase 4 (CDK4) and cyclin dependent kinase 6 (CDK6) expression in BC tumors in the sh-CD47 group had lower levels than that in the control groups (Fig. 5F–I).

4. Discussion

The involvement of *CD47* in cancer research has gained considerable attention since many tumors overexpress this protein to avoid being targeted by the immune system. High levels of *CD47* expression have been correlated with poor prognoses in several malignancies, including breast, prostate, and lung cancers [9,17–19]. Consequently, therapeutic strategies have emerged, such as the development of monoclonal antibodies against *CD47*, which have shown promise for enhancing the phagocytosis of cancer cells in preclinical and clinical trials.

The modulation of *CD47* presents new avenues for therapies aimed at adjusting immune responses in autoimmune conditions. Finally, in infectious diseases, *CD47* may influence the immune response to pathogens, with certain viruses potentially exploiting the *CD47* pathway to evade phagocytosis, thereby prolonging survival in host cells [20]. In summary, *CD47* serves as a critical regulator of the immune response and cellular homeostasis across a spectrum of human diseases. Ongoing research is focused on elucidating its complex role and exploring potential therapeutic interventions that target *CD47* to improve treatment outcomes in various conditions. The *CD47* gene plays a crucial role in the mechanism of malignancies primarily through its functions in immune evasion, tumor growth promotion, and modulation of the tumor microenvironment. As a "don't eat me" signaling protein, *CD47* interacts with *SIRPα* on macrophages, inhibiting phagocytosis and allowing tumor cells to escape immune surveillance [8,10,21]. *CD47* contributes to tumor cell proliferation and survival through various signaling pathways, including integrin signaling, which promotes tumor cell migration and invasion. Moreover, *CD47* affects the tumor microenvironment by regulating the activity and composition of immune cells. It can polarize tumor-associated macrophages towards a pro-tumor phenotype, further aiding tumor progression [22–24]. Therapeutically, *CD47* has emerged as a promising target in cancer immunotherapy, with the development of monoclonal antibodies that block *CD47-SIRPα* interactions, thereby enhancing the phagocytic activity of macrophages against tumor cells. Overall, the multifaceted role of *CD47* in malignancy represents a vital area for ongoing research and potential therapeutic interventions.

The role of *CD47* in BC has emerged as a critical area of research, particularly due to its implications for tumor growth and immune evasion [18,19,25]. Our findings demonstrate that the knockdown of *CD47* significantly decreases the proliferation of BC cells and reduces tumor size in animal models, which is consistent with the existing literature that highlights *CD47*'s essential role in maintaining BC. This conclusion was affirmed by the finding that high *CD47* expression correlated with high *Ki-67* levels. *Ki-67* is a nuclear protein that is associated with cell proliferation [26]. It is widely used as a cellular marker to assess the growth fraction of a given tissue, particularly in tumor pathology. The presence of *Ki-67* in a cell indicates that

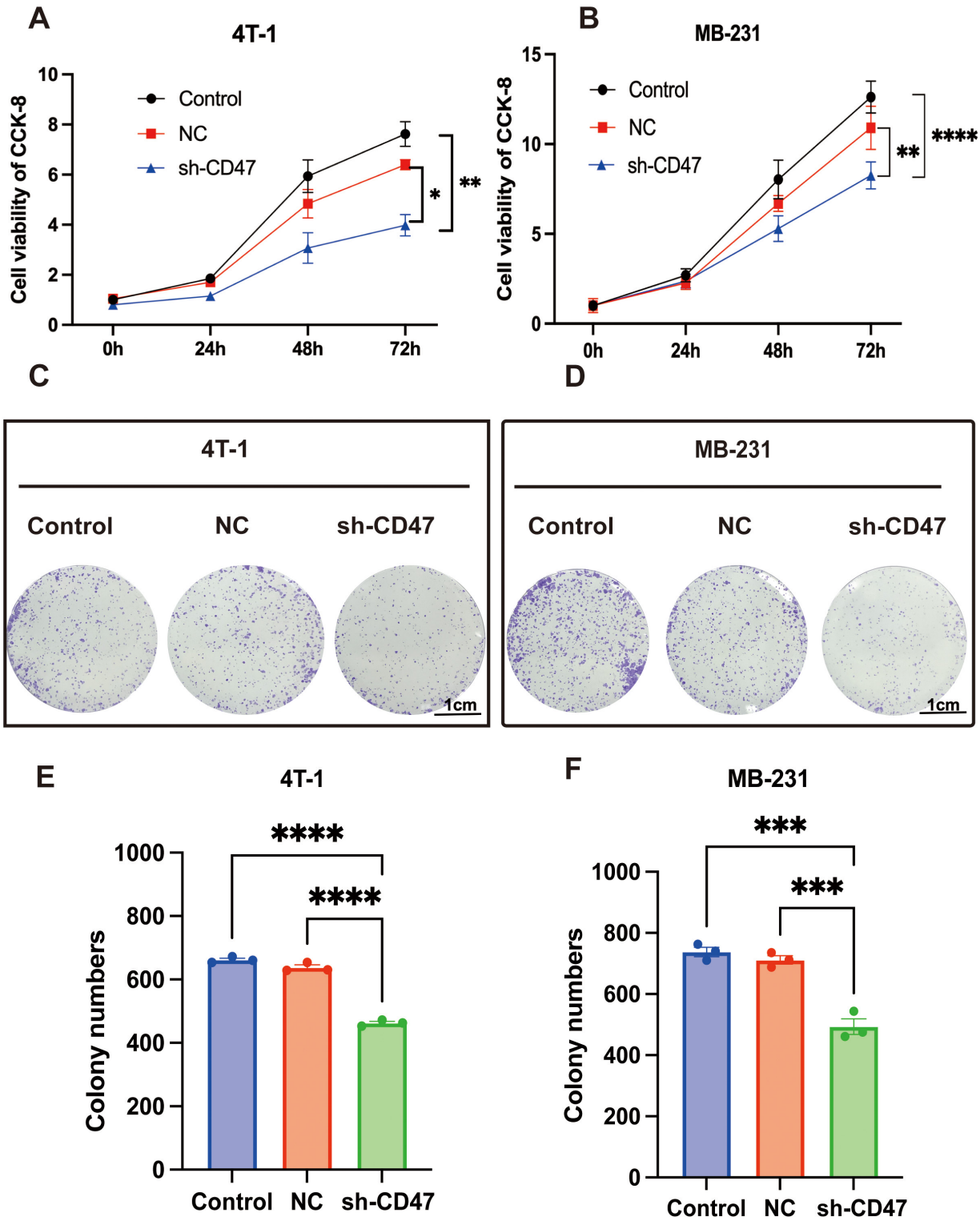

Fig. 3. The functional experiment of *CD47* in breast cancer cells. (A,B) Cell viability of 4T1 and MB-231 cells transfected with short hairpin-CD47, negative control (NC) plasmids were detected by Cell Counting Kit-8 (CCK-8) staining assay. (C–F) Cell monoclonal proliferation of 4T1 and MB-231 cells. The scale bar = 1 cm. *$p < 0.05$, **$p \leq 0.01$, ***$p < 0.001$, ****$p \leq 0.0001$.

it is actively dividing or preparing to divide, making it a valuable tool for evaluating the proliferative activity of tumors [27,28]. Additionally, *CD47* is involved in promoting tumor survival through various signaling pathways, such as the Phosphoinositide 3-kinase/ Protein Kinase B (*PI3K/Akt)* pathway, which enhances cell proliferation and resistance to apoptosis [29].

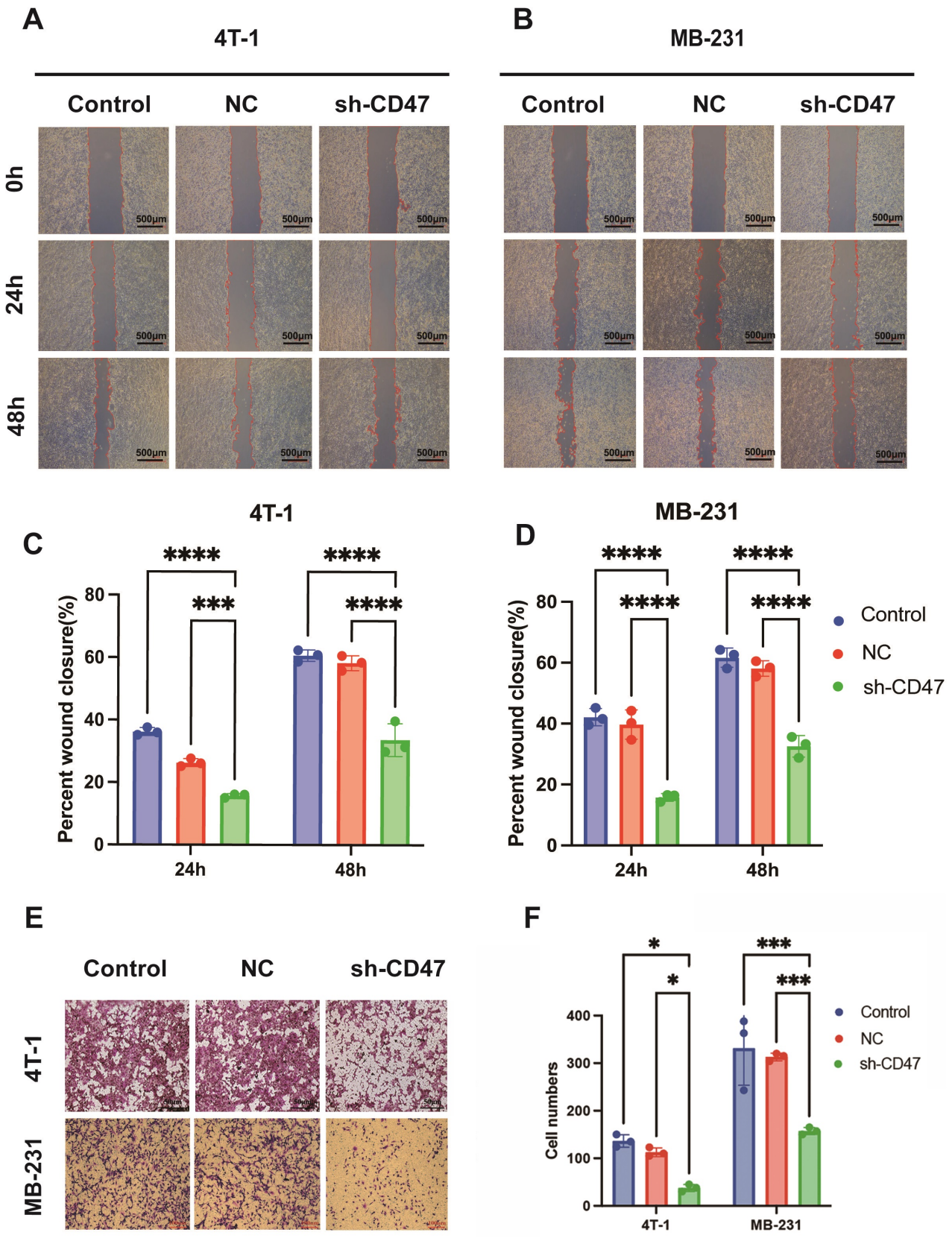

Fig. 4. *CD47* knockdown attenuated the invasion and migration behavior of breast cancer cells. (A–D) Wound healing of 4T1 and MB-231 cells transfected with sh-CD47 and sh-NC plasmids was measured at 24 h and 48 h. The scale bar = 500 μm. (E,F) The transwell detection of 4T1 and MB-231 cells transfected with sh-CD47 and sh-NC plasmids is shown. The scale bar = 50 or 100 μm. *$p < 0.05$, ***$p < 0.001$, ****$p \leq 0.0001$.

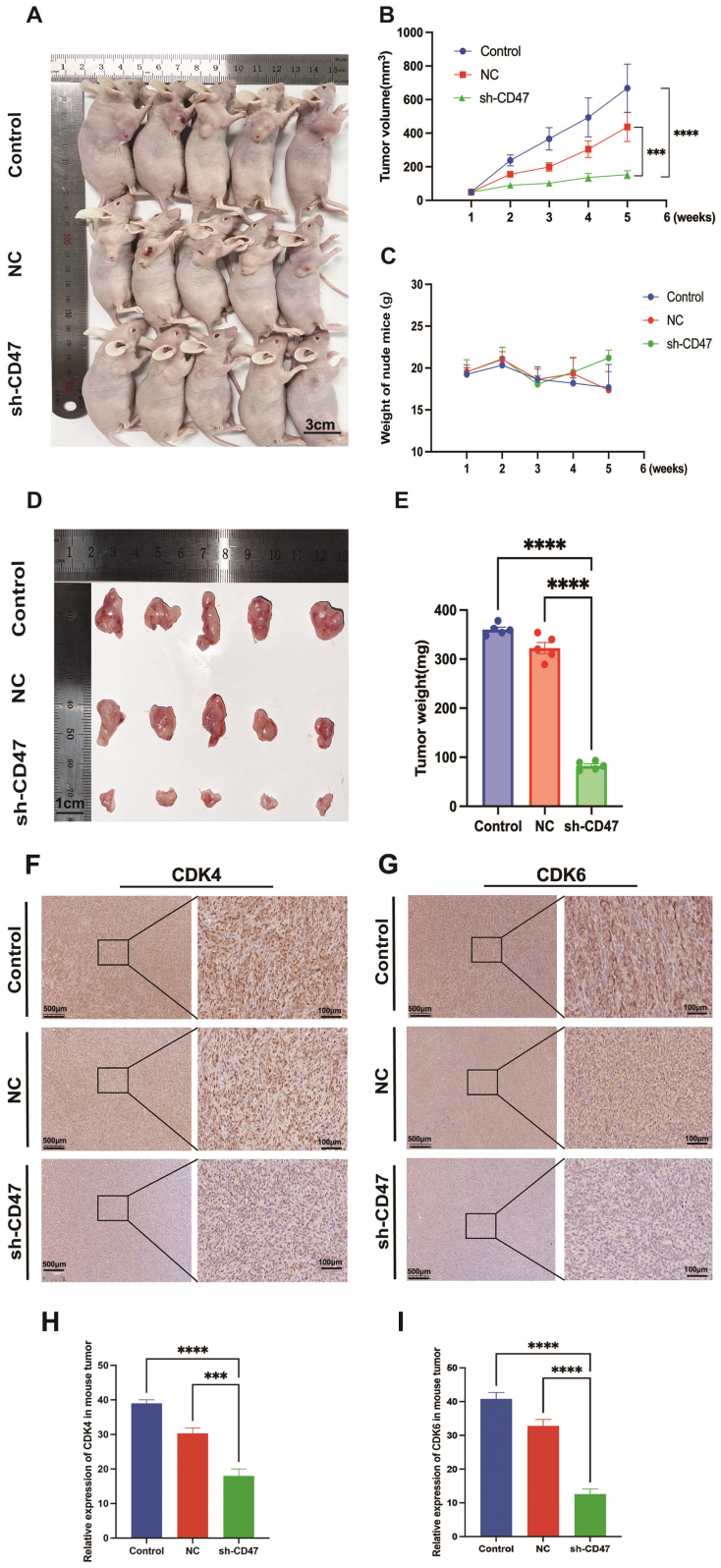

Fig. 5. *CD47* knockdown decreased xenograft tumor volume and weight in nude mice. (A) Gross images of nude mice with BC tumors in the sh-CD47 and control groups. (B,C) Distinct tumor volumes and weights of nude mice are shown. (D,E) The gross species of BC tumors in the sh-CD47 group and the control group are shown; tumor weights were analyzed. (F,G) The cyclin dependent kinase 4/6 expression of BC tumors by immunohistochemistry staining assay. The scale bar = 100 or 500 µm. (H,I) Relative expression values of cyclin dependent kinase 4/6 (n=5). (***$p < 0.001$; ****$p < 0.0001$).

This study centers on the phenotypic impacts of *CD47* in enhancing the proliferation and invasion of BC cells. Nevertheless, we did not examine the fundamental mechanisms through which *CD47* influences these processes, including the activation of cellular signaling pathways. Subsequent research should delve into these internal mechanisms to achieve a more thorough comprehension of *CD47*'s function in BC, potentially facilitating the identification of therapeutic targets.

5. Conclusion

Our study underscores the pivotal role of *CD47* in BC pathogenesis and highlights its dual function in promoting tumor cell propagation. Elevated *CD47* expression in BC tissues, as evidenced by bioinformatics analyses and clinical correlations, is associated with increased *Ki-67* levels, suggesting a direct link to cellular proliferation. Furthermore, findings from *in vitro* and *in vivo* experiments reinforce the critical involvement of *CD47* in maintaining the malignancy of BC cells. The potential of *CD47* as a therapeutic target offers exciting avenues for the development of innovative treatments aimed at enhancing antitumor responses. Future research should focus on elucidating the intricate mechanisms governing *CD47* signaling and exploring the clinical applicability of *CD47*-targeted interventions to improve outcomes in patients with BC.

Declaration of AI and AI-assisted Technologies in the Writing Process

During the preparation of this work the authors used ChatGPT in order to check spell and grammar. After using this tool, the authors reviewed and edited the content as needed and takes full responsibility for the content of the publication.

Availability of Data and Materials

The datasets used and analyzed during the current study can be available from the corresponding author on reasonable request.

Author Contributions

JW (co-first author): Data curation; Investigation; Formal analysis; Methodology. XW (co-first author): Data curation; Methodology; Conception. XL (second corresponding author): Conceptualization; Data curation; supervision. YX (First corresponding author): Conceptualization; Investigation; Resources; Writing—original draft, review and editing; Data curation; Supervision. All authors contributed to editorial changes in the manuscript. All authors read and approved the final manuscript. All authors have participated sufficiently in the work and agreed to be accountable for all aspects of the work.

Ethics Approval and Consent to Participate

The study was approved by the research ethics committee Shandong provincial third hospital (KYLL-2021066 for clinical samples) and registered in Medical Research Registration Information system of China (https://www.medicalresearch.org.cn/). All patients signed informed consent. The study was performed in accordance with the ethical standards as laid down in the 1964 Declaration of Helsinki and its later amendments or comparable ethical standards. All animal experimental processes were approved by the Laboratory Animal Center of Shandong Third Hospital (No. DWKYLL-2021023 for animal models). The study is reported in accordance with ARRIVE guidelines of experimental animals.

Acknowledgment

Not applicable.

Funding

(1) Science and Technology Development Program of Shandong Geriatrics Society (LKJGG2021Z005); (2) Scientific research cultivation fund of Shandong provincial third hospital (M2023004/sjzd004); (3) Medical and Health Science and Technology Project of Shandong Province (2023BJ000037).

Conflict of Interest

The authors declare no conflict of interest.

Supplementary Material

Supplementary material associated with this article can be found, in the online version, at https://doi.org/10.31083/FBL28210.

References

[1] Benitez Fuentes JD, Morgan E, de Luna Aguilar A, Mafra A, Shah R, Giusti F, *et al*. Global Stage Distribution of Breast Cancer at Diagnosis: A Systematic Review and Meta-Analysis. JAMA Oncology. 2024; 10: 71–78. https://doi.org/10.1001/jamaoncol.2023.4837.

[2] Ge A, He Q, Zhao D, Li Y, Chen J, Deng Y, *et al*. Mechanism of ferroptosis in breast cancer and research progress of natural compounds regulating ferroptosis. Journal of Cellular and Molecular Medicine. 2024; 28: e18044. https://doi.org/10.1111/jcmm.18044.

[3] Kundu M, Butti R, Panda VK, Malhotra D, Das S, Mitra T, *et al*. Modulation of the tumor microenvironment and mechanism of immunotherapy-based drug resistance in breast cancer. Molecular Cancer. 2024; 23: 92. https://doi.org/10.1186/s12943-024-01990-4.

[4] Kleiblová P, Novotný J, Cibula D, Curtisová V, Dubová O, Foretová L, *et al*. The guidelines for clinical practice for carriers of germline mutations in hereditary breast, ovarian, prostate, and pancreatic cancer predisposition genes BRCA1, BRCA2, PALB2, ATM, and CHEK2 (4.2024). Klinicka Onkologie: Casopis Ceske a Slovenske Onkologicke Spolecnosti. 2024; 38: 292–299. https://doi.org/10.48095/ccko2024292.

[5] Dogan I, Ahmed MA, Yıldız A, Vatansever S. Rechallenge of Trastuzumab-based Therapy in HER2-Positive Breast Cancer Patients who Progressed Under TDM-1. Indian Journal of Surgical Oncology. 2024; 15: 484–488. https://doi.org/10.1007/s13193-024-01935-9.

[6] Liu Y, Weng L, Wang Y, Zhang J, Wu Q, Zhao P, *et al*. Deciphering the role of CD47 in cancer immunotherapy. Journal of Advanced Research. 2024; 63: 129–158. https://doi.org/10.1016/j.jare.2023.10.009.

[7] Zhang T, Wang F, Xu L, Yang YG. Structural-functional diversity of CD47 proteoforms. Frontiers in Immunology. 2024; 15: 1329562. https://doi.org/10.3389/fimmu.2024.1329562.

[8] Zhao P, Xie L, Yu L, Wang P. Targeting CD47-SIRPα axis for Hodgkin and non-Hodgkin lymphoma immunotherapy. Genes & Diseases. 2023; 11: 205–217. https://doi.org/10.1016/j.gendis.2022.12.008.

[9] Chuang CH, Zhen YY, Ma JY, Lee TH, Hung HY, Wu CC, *et al*. CD47-mediated immune evasion in early-stage lung cancer progression. Biochemical and Biophysical Research Communications. 2024; 720: 150066. https://doi.org/10.1016/j.bbrc.2024.150066.

[10] Huang C, Wang X, Wang Y, Feng Y, Wang X, Chen S, *et al*. Sirpα on tumor-associated myeloid cells restrains antitumor immunity in colorectal cancer independent of its interaction with CD47. Nature Cancer. 2024; 5: 500–516. https://doi.org/10.1038/s43018-023-00691-z.

[11] Zhang K, Xu Y, Chang X, Xu C, Xue W, Ding D, *et al*. Co-targeting CD47 and VEGF elicited potent anti-tumor effects in gastric cancer. Cancer Immunology, Immunotherapy. 2024; 73: 75. https://doi.org/10.1007/s00262-024-03667-9.

[12] Wilson KJ, Roldán-Nofuentes JA, Henrion MYR. testCompareR: an R package to compare two binary diagnostic tests using paired data. Wellcome Open Research. 2024; 9: 351. https://doi.org/10.12688/wellcomeopenres.22411.3.

[13] Kanehisa M, Furumichi M, Sato Y, Kawashima M, Ishiguro-Watanabe M. KEGG for taxonomy-based analysis of pathways and genomes. Nucleic Acids Research. 2023; 51: D587–D592. https://doi.org/10.1093/nar/gkac963.

[14] Sato N, Uematsu M, Fujimoto K, Uematsu S, Imoto S. ggkegg: analysis and visualization of KEGG data utilizing the grammar of graphics. Bioinformatics. 2023; 39: btad622. https://doi.org/10.1093/bioinformatics/btad622.

[15] Schneider CA, Rasband WS, Eliceiri KW. NIH Image to ImageJ: 25 years of image analysis. Nature Methods. 2012; 9: 671–675. https://doi.org/10.1038/nmeth.2089.

[16] Cicero L, Fazzotta S, Palumbo VD, Cassata G, Lo Monte AI. Anesthesia protocols in laboratory animals used for scientific purposes. Acta Bio-Medica: Atenei Parmensis. 2018; 89: 337–342. https://doi.org/10.23750/abm.v89i3.5824.

[17] Wang Q, Feng C, Chen Y, Peng T, Li Y, Wu K, *et al*. Evaluation of CD47 in the Suppressive Tumor Microenvironment and Immunotherapy in Prostate Cancer. Journal of Immunology Research. 2023; 2023: 2473075. https://doi.org/10.1155/2023/2473075.

[18] Chantaraamporn J, Pothipan P, Sakulterdkiat T, Khiankaew B, Lumkul L, Mutapat P, *et al*. CD47 and Calreticulin Expression in Breast Cancer Subtypes and Anti-CD47 Inhibitory Effects in Macrophage-mediated Phagocytosis. Anticancer Research. 2024; 44: 4929–4940. https://doi.org/10.21873/anticanres.17318.

[19] Zhang B, Shi J, Shi X, Xu X, Gao L, Li S, *et al*. Development and evaluation of a human CD47/HER2 bispecific antibody for Trastuzumab-resistant breast cancer immunotherapy. Drug Resistance Updates. 2024; 74: 101068. https://doi.org/10.1016/j.drup.2024.101068.

[20] Zuo H, van Lierop MJC, Kaspers J, Bos R, Reurs A, Sarkar S, *et al*. Transfer of Cellular Content from the Allogeneic Cell-Based Cancer Vaccine DCP-001 to Host Dendritic Cells Hinges on Phosphatidylserine and Is Enhanced by CD47 Blockade. Cells. 2021; 10: 3233. https://doi.org/10.3390/cells10113233.

[21] Hutter G, Theruvath J, Graef CM, Zhang M, Schoen MK, Manz EM, *et al*. Microglia are effector cells of CD47-SIRPα antiphagocytic axis disruption against glioblastoma. Proceedings of the National Academy of Sciences of the United States of America. 2019; 116: 997–1006. https://doi.org/10.1073/pnas.1721434116.

[22] Dawoud MM, Abd El Samie Aiad H, Kasem NS, El Khouly EAB, Al-Sharaky DR. Is overexpression of CD163 and CD47 in tumour cells of breast carcinoma implicated in the recruitment of tumour-associated macrophages (TAMs) in tumour microenvironment? immunohistochemical prognostic study. Journal of Immunoassay & Immunochemistry. 2024; 45: 342–361. https://doi.org/10.1080/15321819.2024.2358879.

[23] Gautam PK, Acharya A. Suppressed expression of homotypic multinucleation, extracellular domains of CD172α (SIRP-α) and CD47 (IAP) receptors in TAMs upregulated by Hsp70-peptide complex in Dalton's lymphoma. Scandinavian Journal of Immunology. 2014; 80: 22–35. https://doi.org/10.1111/sji.12180.

[24] Lu J, Li J, Lin Z, Li H, Lou L, Ding W, *et al*. Reprogramming of TAMs via the STAT3/CD47-SIRPα axis promotes acquired resistance to EGFR-TKIs in lung cancer. Cancer Letters. 2023; 564: 216205. https://doi.org/10.1016/j.canlet.2023.216205.

[25] Tong S, Zhu Y, Leng Y, Wu Y, Xiao X, Zhao W, *et al*. Restoration of miR-299-3p promotes macrophage phagocytosis and suppresses malignant phenotypes in breast cancer carcinogenesis via dual-targeting CD47 and ABCE1. International Immunopharmacology. 2024; 130: 111708. https://doi.org/10.1016/j.intimp.2024.111708.

[26] Ding Z, Hagan M, Yan F, Schroer NWY, Polmear J, Good-Jacobson KL, *et al*. Ki67 deficiency impedes chromatin accessibility and BCR gene rearrangement. The Journal of Experimental Medicine. 2024; 221: e20232160. https://doi.org/10.1084/jem.20232160.

[27] Ramos-Santillan V, Oshi M, Nelson E, Endo I, Takabe K. High Ki67 Gene Expression Is Associated With Aggressive Phenotype in Hepatocellular Carcinoma. World Journal of Oncology. 2024; 15: 257–267. https://doi.org/10.14740/wjon1751.

[28] Sprenger F, da Silva Junior EB, Ramina R, Cavalcanti MS, Martins SB, Cerqueira MA, *et al*. Ki67 Index Correlates with Tumoral Volumetry and 5-ALA Residual Fluorescence in Glioblastoma. World Neurosurgery. 2024; 189: e230–e237. https://doi.org/10.1016/j.wneu.2024.06.023.

[29] Liu Y, Chang Y, He X, Cai Y, Jiang H, Jia R, *et al*. CD47 Enhances Cell Viability and Migration Ability but Inhibits Apoptosis in Endometrial Carcinoma Cells via the PI3K/Akt/mTOR Signaling Pathway. Frontiers in Oncology. 2020; 10: 1525. https://doi.org/10.3389/fonc.2020.01525.